Science & Technology Development Journal 2022, 25(4):2573-2580

Open Access Full Text Article

Research article

Establishment of a fiber optic sensor coupled to the plasmonic effect of silver nanoparticles in glucose concentration monitoring

Nguyen Tran Truc Phuong[1,2], Vinh Quang Dang[1,2], Hanh Kieu Thi Ta[1,2], Ngoc Xuan Dat Mai[2,3], Anh Tuan Thanh Pham[2,4], Dung Van Hoang[2,4], Nhu Hoa Thi Tran[1,2,*]

ABSTRACT

Introduction: Diabetes is an extremely dangerous disease due to the disorder of glucose metabolism in the body leading to serious complications and the cause of other dangerous diseases. Therefore, the continuous monitoring of glucose levels in the body is particularly important in the prevention and treatment of this disease. Optical fiber sensors that apply the LSPR effect of silver nanoparticles show great potential in the field of sensors that enable precise label-free monitoring of analyte concentrations with high sensitivity, which is receiving much attention. **Methods:** The sensitivity of the LSPR effect on the surface of AgNPs to the dielectric properties of the medium, namely, the refractive index of the analyte solution, was determined. Variation in the LSPR conditions of AgNPs leads to either donation or reduction in optical power. Based on that mechanism, the fiber was used as a waveguide and immobilized on a self-assembled monolayer of the AgNP 1 core surrounded by a microfluidic channel that allows the analyte solution to pass through the sensing area through a biological pump. This process of changing the capacity allows the assessment of glucose concentration in solution to a very small degree of change. **Results:** AgNPs of approximately 90 nm in size were quickly and simply synthesized with high stability and uniformity by chemical reduction with an ethylene glycol reducing agent, as demonstrated by FESEM and DLS results. The LSPR wavelength of the AgNP solution observed by the UV–vis spectrum is 435 nm. At the same time, a fiber-optic sensor system that monitors glucose concentration changes has also been successfully established with a sensitivity of 0.025 RIU corresponding to a detection limit (LOD) of up to 0.35 mM. **Conclusions:** An optical fiber optical sensor based on the LSPR phenomenon of AgNPs was initially established and showed high sensitivity in detecting and monitoring changes in glucose concentration without the use of complex markers or enzymes. The compact size of the fiber sensor opens up the potential for integration into handheld optical devices to help monitor health more proactively.

Key words: Silver nanoparticles, LSPR, glucose sensor, optical sensor, detection of limited

[1]*Faculty of Materials Science and Technology, University of Science, Ho Chi Minh City, Viet Nam*

[2]*Vietnam National University, Ho Chi Minh City, Viet Nam*

[3]*Center for Innovative Materials and Architectures (INOMAR), HoChiMinh City, Viet Nam*

[4]*Laboratory of Advanced Materials, University of Science, HoChiMinh City, Viet Nam*

Correspondence

Nhu Hoa Thi Tran, Faculty of Materials Science and Technology, University of Science, Ho Chi Minh City, Viet Nam

Vietnam National University, Ho Chi Minh City, Viet Nam

Email: ttnhoa@hcmus.edu.vn

History

- Received: 2022-08-04
- Accepted: 2023-01-06
- Published: 2023-01-20

DOI : 10.32508/stdj.v25i4.3984

INTRODUCTION

Silver nanoparticles are widely known for their excellent bactericidal ability, and they have increasingly become a bright star among metal nanoparticles thanks to their irreplaceable applications based on the powerful electromagnetic field generated by the LSPR effect. Various synthesis methods have been studied and applied to quickly and easily and stably fabricate silver nanoparticles, such as chemical reduction [1,2], biogenic synthesis [3,4], microwave use [5], irradiation [6], and electrochemical synthesis [7]. Each method has its own highlights, and the chemical reduction method is of particular interest because of its suitable advantages to develop and produce AgNPs with different morphologies and sizes that are quick and convenient without requiring expensive bulky equipment. The morphology and size of AgNPs depend greatly on the reaction conditions, such as the concentration of the reactants, reaction temperature, stirring rate, and pH [8,9], and the plasmon peak of AgNPs depends greatly on the morphology and size of AgNPs. Therefore, controlling the maximum absorption wavelength of AgNPs becomes simpler than ever by investigating the immobilization of these factors.

In recent years, optical sensors have attracted increasing attention because of their features that meet the needs of modern society with extremely high sensitivity and compactness. Much research has been conducted on sensors such as fluorescence [10], NIR spectroscopy [11], Raman spectroscopy [12], and optical sensors using the LSPR effect [13], which are interested in developing applications in many different fields. Especially in biomedical molecule detection, health monitoring has some examples that can be mentioned as the LSPR sensor system developed by M.H. Tu *et al.* [14] established the strong plasmonic effect of hollow gold nanoparticles immobilized on fibers, which

Cite this article : Phuong N T T, Dang V Q, Ta H K T, Mai N X D, Pham A T T, Hoang D V, Tran N H T. **Establishment of a fiber optic sensor coupled to the plasmonic effect of silver nanoparticles in glucose concentration monitoring**. *Sci. Tech. Dev. J.; 2022,* 25(4):2573-2580.

were used as probes. This sensor system obtained satisfactory results in terms of sensitivity when reaching 1933 nm/RIU. In another study by Vu Thi Huong *et al.*[13], who established a fiber-based optical sensor system applying the plasmonic effect of gold nanoparticles to detect bovine serum albumin molecules, many remarkable results were obtained, except that the detection limit reached 0.0075 ng/ml. In this study, we developed a fiber-based optical sensing system combined with AgNPs to create a sensing region that is sensitive to changes in the refractive index of the analyte solution. The strong LSPR effect of AgNPs enhances the sensor's sensitivity to the medium's refractive index through the sensitivity of the LSPR peak.
Glucose was used by us as a probe molecule for the sensor. This is a common, available, nontoxic substance, but it has great biological significance, participating in most of the metabolic processes in the body in many different forms. Detecting and monitoring the concentration of glucose in the body plays a particularly important role in health care. Disordered glucose metabolism is the main cause of diabetes, an extremely dangerous disease with many serious complications that lead to heart failure, kidney failure, and eye problems. This disease has the third highest mortality rate in the world after cancer and heart disease. For that reason, we have conducted experimental development of a fiber-optic optical sensor system that combines the LSPR effect of AgNPs in detecting and monitoring glucose concentration. We hope that the results obtained in this study will pave the way for the development of small, highly sensitive sensor systems that can monitor glucose levels in the body in real time and noninvasively through saliva and respiratory fluid.

MATERIALS AND METHODS

Materials and reagents

Silver nitrate ($AgNO_3$, 99%), polyvinylpyrrolidone (PVP, $M_w \sim 55000$, and (3-aminopropyl) triethoxysilane (APTES, 99%) were purchased from Sigma Aldrich. Ethylene glycol (EG, $C_2H_6O_2$), sodium sulfide nonahydrate natri sulfide ($Na_2S.9H_2O$, > 98%), and sodium hydroxide (NaOH, 96%) were supplied by Guangdong Guanghua Sci-Tech Co., Ltd. (China). Ethanol (EtOH, C_2H_5OH, 99.8%) and D-glucose ($C_6H_{12}O_6$) were provided by Fisher Ltd. (UK). Polydimethylsiloxane (PDMS, Sylgard 184, Dow Corning Co., USA). The sensor is assembled by aligning a multimode optical fiber (numerical aperture of 0.37, JFTLH-Polymicro Technologies) with a core diameter of 200 μm.

Preparation of silver nanoparticles (Ag NPs)

AgNPs were synthesized through a chemical reduction reaction with an ethylene glycol reducing agent according to the following procedure: a 25 ml 3-necked flask containing 15 ml of EG and 90 mg of PVP was heated to 170 °C. Then, 70 μl of Na_2S solution was added, and at the same time, 1 ml of 96 mg $AgNO_3$ in EG was also added. The reaction was maintained for 100 minutes and quenched by an ultrasonic bath in 5 mins. The circulation system and magnetic stirring were maintained throughout the reaction. Finally, residual PVP and EG were removed by centrifugation several times with DI water and acetone, and then AgNPs were redispersed in 30 ml of DI water and stored at 4 °C.

Fiber (SiO_2) modification of silver nanoparticles (Ag NPs)

The process of functionalizing AgNPs on SiO_2 substrates was performed similarly based on the research paper of Vu Thi Huong *et al.*[15]. First, the two ends of the multimode fiber are attached to the FC/PC connection device then, a segment in the middle of the fiber is removed from both the jacket and the cladding layer. The core exposed after the removal process was denatured in turn with the -OH functional group by the oxygen plasma machine (CUTE-1MPR, Femto Science Inc., Korea) to create -OH groups on the surface of the sample. Next, the core of this fiber is soaked in APTES 3% solution to create an NH_2 functional group. Finally, after undergoing 2 rounds of denaturation, the core was soaked in AgNP solution for 2 h to produce an AgNP sensing layer.

The optical fiber sensor system

The manufacturing process of the LSPR microfluidic PDMS sensor and optical real-time measurement system is similar to that of a previous study[15]. The optical system is depicted in **Figure 1**.

Analytical Methods

The AgNPs were evaluated for optical properties by V-730 ultraviolet–visible spectroscopy (UV–Vis) from JASCO in the 300 to 900 nm wavelength region in conjunction with ZS90 dynamic light scattering (DLS) from Malvern Panalytical, the UK, to determine the particle size distribution in solution. The surface modification in preparation for the immobilization of Ag nanoparticles and the coating properties was also demonstrated through a series of analyses such as Fourier transform infrared spectroscopy

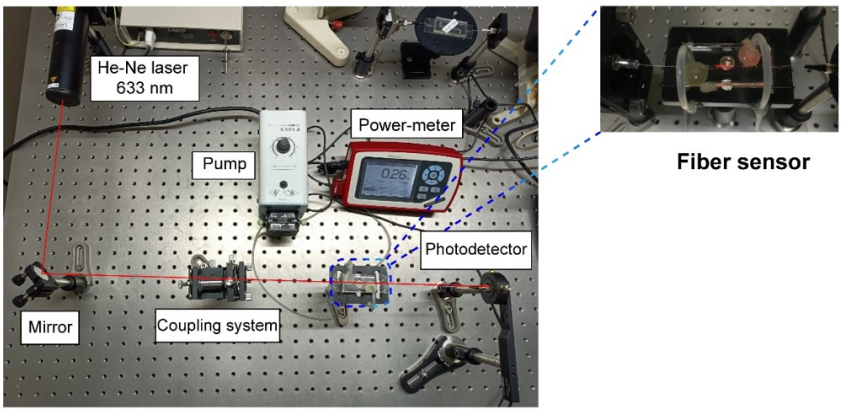

Figure 1: Image of the fiber optic sensor system set up at the Center for Innovative Materials and Architectures (INOMAR), Vietnam National University, Ho Chi Minh City (VNU-HCM).

(FTIR) by the Vertex 70v in transmission mode between 4000 cm^{-1} and 500 cm^{-1}; the Phoenix 300 water contact angle supplied by Surface Electro-Optics, Korea; powder X-ray diffraction (PXRD) Ni-filtered Cu Kα (λ = 1.541 78 Å) radiation operated at 40 kV and 40 mA (1600 W) in the range of 30–80°; the Hitachi 4800 field emission scanning electron microscope (FESEM) at the scale of 1 μm.

RESULTS

The AgNP solution with a green orchest color and good dispersion in DI solvents was evaluated for its optical properties through UV–vis absorption spectroscopy, as shown in **Figure 2**a, which shows the plasmon peak at 435 nm and size distribution. The size of the particles in the solution was demonstrated by DLS spectroscopy, showing an average size of 119 nm, as shown in **Figure 2**b.

The glass substrate surface is in turn modified for the final purpose of immobilizing AgNPs through the NH_2 functional group. Each denaturation step was checked by measuring the water contact angle and FTIR spectroscopy to ensure that the denaturation was successful, and the results are shown in Figure 3. The properties of crystal structure and purity are demonstrated in the XRD results investigated in the 2-theta angle range from 30 to 80 degrees in 1, 2, and 4 h samples. The results are shown in **Figure 4**a. After surface modification to form the NH_2 group, the substrates were soaked in AgNP solution for 1, 2, and 4 h. The density of the AgNPs on the surface is depicted in the surface FESEM in **Figure 4** b-d.

D-glucose solution with 14 different concentrations from 0 to 20 mM was continuously directed through the microfluidic channel through a biological pump (EYELA, SMP-21) to fix the flow rate. The output power was recorded with a retention time of 60 s corresponding to 60 data points for each concentration. The resulting power output change for the added concentrations of d-glucose is shown in **Figure 5**.

DISCUSSION

AgNPs are fabricated by the polyol reduction method using EG as a reducing agent combined with PVP to stabilize the surface and capping agent because the effective adhesion of PVP to the surface (100) of the reduced Ag nuclei will be easily development-oriented (111). At the same time, Na_2S acts as a corrosive agent for the corners of AgNP bars, creating polygonal Ag particles, which is explained by the appearance of a small ridge at 370 nm. The plasmon peaks of AgNPs observed at 435 nm were highly balanced, showing the uniformity in size and shape of the particles in the solution (**Figure 2**a). This hypothesis is further supported by the results of the DLS spectrum shown in **Figure 2**b. From the DLS spectrum, it can be observed that the particles are mainly concentrated in diameter in the range of 80 – 120 nm, and the average size is calculated as 119 nm.

Immobilization of AgNPs through NH_2 functional groups has been demonstrated previously however, a number of analyses were still performed to verify that was performed. First, the glass surface that has not undergone any modification has a wetting angle of 63.5 $\pm$ 0.3 degrees. After this surface was treated with oxygen plasma for 2 min, the contact angle was reduced to approximately 12.0 $\pm$0.5 degrees. This shows that the oxygen plasma environment created

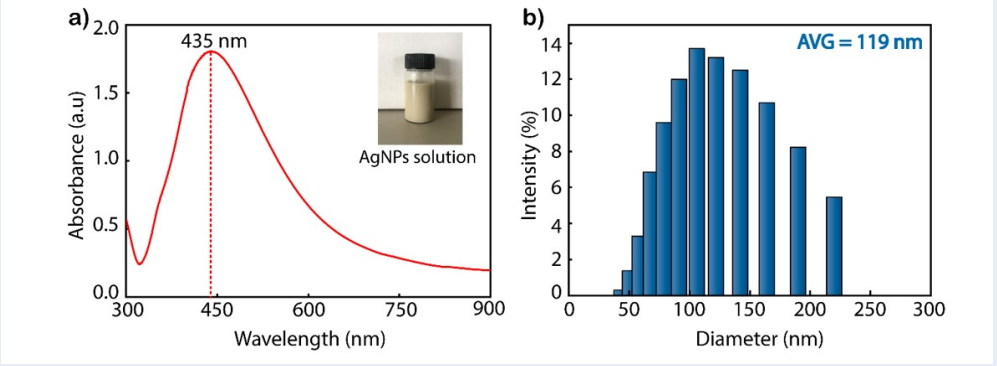

Figure 2: UV–vis spectrum (a) and DLS spectrum (b) of AgNP solution.

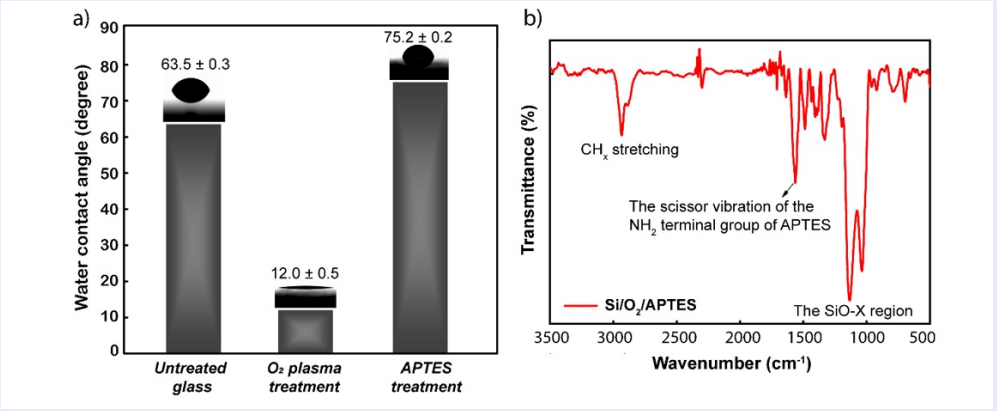

Figure 3: Schematic depicting the change in contact angle through surface modifications (a) and FTIR spectra of the substrate surface after APTES modification (b).

very hydrophilic free OH^- groups on the glass substrate. Continuing the glass substrate after 2 turns of surface transformation, which is plasma oxygen and immersed in 3% APTES solution, the contact angle has increased from 12 ± 0.5 to 75.2 ±0.2 degrees. The -NH_2 groups are hydrophilic, but in this case, the contact angle increased from 12 ±0.5 to 75 ±0.2 degrees, which is explained by the hydrogen bonding effect that occurs between the OH^- groups formed due to the hydroxylated substrate surface and the NH^- group formed from amine functionalization, thus causing an increase in the contact angle even though NH_2 is hydrophilic [16] (**Figure 3**a). FTIR analysis is a confirmation of the successful function of the NH_2 functional group on the surface of the glass substrate. Specifically, in **Figure 3**b, the appearance of the scissor vibration of the NH_2 terminal group of APTES at the band 1570 cm^{-1} can be observed.

The AgNP particles have good crystallinity, mainly growing in the (111) orientation [17], as shown by the characteristic diffraction peak of Ag at an angle of 2 to 38.16 degrees in the XRD diagram (**Figure 4**a). The crystal size is 350 nm, which is calculated by the Scherrer formula $d = \frac{k\lambda}{\beta \cos(\theta)}$, where d is the grain size, k (shape factor in the case of spherical nanoparticles) is used with a value of 0.9, λ is the wavelength of the X-ray radiation used, β is the full width at half maximum (FWHM), and θ is the Bragg angle. In addition, this result also partly proves that the AgNP coating is completely pure without any change in the crystal structure. Increasing the immersion time makes the AgNP layer have a higher density but does not change the properties of the particles, which is observed by the intensity donation of the XRD diffraction peak when examined at times 1, 2, and 4 h without any other changes being observed. The density of AgNPs immobilized onto glass substrates is highly dependent on the time these substrates are immersed in AgNP solution. Specifically, observing

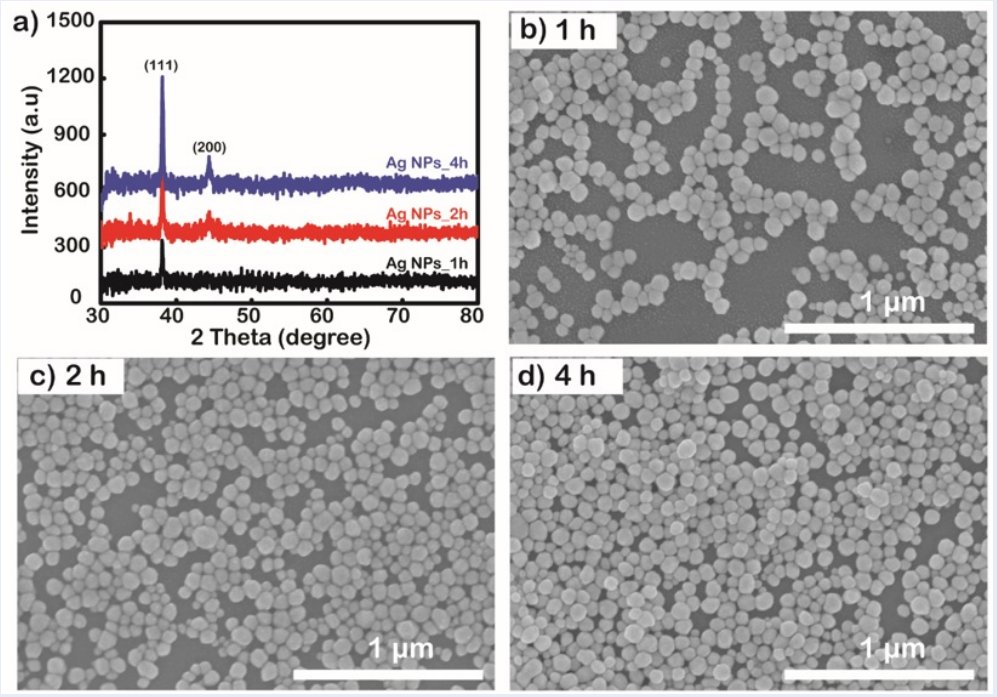

Figure 4: a) XRD pattern of the investigated AgNP coatings by immersion times of 1, 2, and 4 h. b), c), and d) FESEM images of substrate surfaces after immobilization of AgNPs by solution immersion times of 1, 2, and 4 h, respectively.

the FESEM images (**Figure 4**b-d) over the time of the investigated samples according to immersion times of 1, 2, and 4 h, it is very clear that the 1 h sample has a low density and AgNPs have a higher density as the soaking time increases. The diameter of AgNPs calculated from FESEM images is approximately 90 nm and has high homogeneity. At the longest survey period of 4 h, it was observed that the superposition of AgNPs on top of each other makes the uniformity on the surface not guaranteed and well controlled. Homogeneous monolayer Ag coatings with high density have been shown to have good sensitivity to environmental conditions therefore, in this case, a 2 h coating was selected for the glucose assay.

Self-assembled AgNP coating with a 2 h immersion time observed for good surface coverage is a suitable choice for fiber application, allowing the sensor system's sensitivity to increase significantly in response to the LSPR effect, and the surface effect is maximized [18]. The sensitivity of the absorptive peaks of precious metal nanoparticles to specific environmental factors in this case, the refractive index of the analyte solution, has been demonstrated previously by many previous studies [19,20]. When the laser light source passes through the fiber optic sensor, the light will stimulate the LSPR effect of the AgNPs. When light interacts with AgNPs, a part will be absorbed or scattered by AgNPs, which is observed by the transmitted power spectrum. LSPR has a close relationship with the dielectric properties of the medium in contact with the metal surface, so it is very sensitive to changes in RI ($\triangle n$) caused by different concentrations of analytes. Even a very small change in the surface of the dielectric metal can cause a change in the output power of the system because changes in LSPR conditions lead to changes in the absorbance of the wavelength. The relationship between the change in refractive index ($\triangle n$) and the change in wavelength ($\triangle \lambda_{max}$) in the damping of the nanostructure is roughly described as [21]:

$$\triangle \lambda_{max} = m(\triangle n)\left[1 - e^{\left(-\frac{2d}{l_d}\right)}\right]$$

where m is the sensitivity factor, $\triangle n = n_{adsorbate} - n_{medium}$ is the variability in the RI near the metallic surface, d is the thickness of the effective adsorbent layer on the surface sensing, and l_d is the decay length of the electromagnetic field [22]. The schematic diagram depicting the variation in power output with the injection of glucose concentrations from 0 to 20

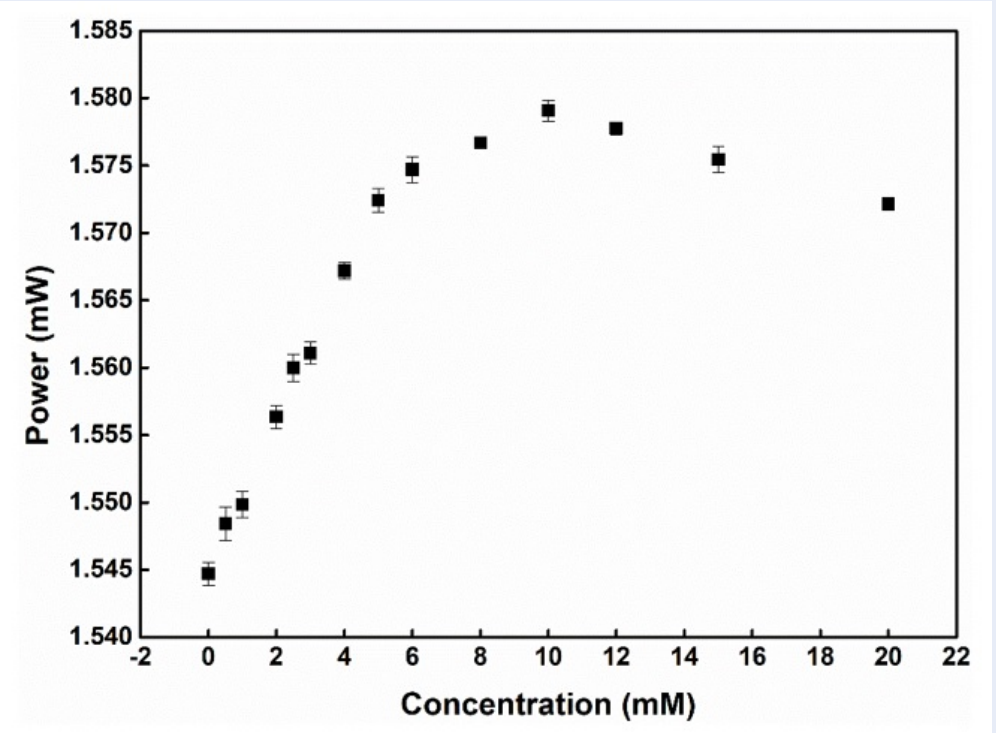

Figure 5: Graph showing the dependence of the output power on the concentration of d-glucose continuously transmitted through the microfluidic channel.

mM sequentially in **Figure 5** shows that power output in the period from 0 to 10 mM causes a continuous increase in the output power. This result suggests that there is a blueshift of the extinction spectra for the change in the refractive index induced by the change in glucose concentration. This change causes the absorbance for the excitation wavelength at 633 nm to decrease, which may be the main cause of the increase in the output optical power compared to the original. The output optical power no longer depends only on the change in the LSPR effect caused by the change in the dielectric properties of the metal surface but also on the difference in the numerical aperture, which is calculated according to the formula $NA = \sqrt{n_{core}^2 - n_{clad}^2}$. Increasing the refractive index of the analyte solution reduces the NA difference when passing light from the sensing region through the waveguide, thereby increasing the output power. When the concentration of glucose becomes too large from 10 to 20 mM, the decrease in the output optical power observed in **Figure 5** due to the increase in refractive index gradually slows down and begins to saturate while the glucose concentration increases. The light absorption capacity of the solution also gradually increases, leading to a decrease in optical power. The detection limit of the fiber optic sensor system is calculated as 0.35 mM, corresponding to a sensitivity value of 0.025 RIU. This is a positive result for the initial setup of an optical sensor system for glucose.

CONCLUSIONS

In this study, we have successfully built a label-free sensor system for glucose by taking advantage of the sensitivity of the LSPR effect on AgNPs to the properties of the dielectric medium in contact with the surface of AgNPs. The new and outstanding feature of this sensor system is that there is no need to use markers or specific enzymes such as glucose oxidase. This makes the system simpler and easier to integrate into portable healthcare monitoring devices. With a measured initial detection limit of 0.35 mM corresponding to a sensitivity of 0.025 RIU, and this number can still achieve better values when the system is optimized, the sensor system promises to unlock many potential applications not only in the field of healthcare but also in other fields.

ABBREVIATIONS

PVP: polyvinylpyrrolidone
APTES: 3-(Triethoxysilyl)Propylamine

EG: ethylene glycol
PDMS: Polydimethylsiloxane
Ag NPs: silver nanoparticles
LOD: detection of limited
XRD: X-ray diffraction
DLS: dynamic light scattering
FESEM: field emission scanning electron microscopy (FESEM)
FTIR: Fourier transform infrared spectroscopy
UV–vis: Ultraviolet–visible spectroscopy

COMPETING INTEREST

The author(s) declare that they have no competing interests.

AUTHORS' CONTRIBUTION

All the authors read and corrected the submitted final version.

Nguyen Tran Truc Phuong conceived the experimental design, analyzed the data, and wrote the manuscript with support from Dr. Nhu Hoa Thi Tran. Vinh Quang Dang, Hanh Kieu Thi Ta, and Ngoc Xuan Dat Mai carried out the experiments in groups.

Anh Tuan Thanh Pham and Dung Van Hoang supported the analysis techniques. Dr. Nhu Hoa Thi Tran revised and corrected the manuscript.

ACKNOWLEDGEMENT

This research is funded by Vietnam National University Ho Chi Minh City (VNU-HCM) under grant number DS2022-18-01.

REFERENCES

1. Suriati G, Mariatti M, Azizan A. Synthesis of silver nanoparticles by chemical reduction method: effect of reducing agent and surfactant concentration. Int J Automot Mech Eng. 2014; ISSN:1920-7;Available from: https://doi.org/10.15282/ijame.10.2014.9.0160.
2. Quintero-Quiroz C, Acevedo N, Zapata-Giraldo J, Botero LE, Quintero J, Zárate-Trivinõ D, et al. Optimization of silver nanoparticle synthesis by chemical reduction and evaluation of its antimicrobial and toxic activity. Biomater Res. 2019; 23(1):1-15;PMID: 31890269. Available from: https://doi.org/10.1186/s40824-019-0173-y.
3. Ahmad N, Fozia, Jabeen M, Haq ZU, Ahmad I, Wahab A, et al. Green fabrication of silver nanoparticles using euphorbia serpens kunth aqueous extract, their characterization, and investigation of its in vitro antioxidative, antimicrobial, insecticidal, and cytotoxic activities. Biomed Res Int. 2021; 2022:1-10;PMID: 35047637. Available from: https://doi.org/10.1155/2022/5562849.
4. Raj S, Trivedi R, Soni V. Biogenic synthesis of silver nanoparticles, characterization and their applications. Surface Modification of Nanoparticles for Biomedical Applications. 2022,;5(1):67-90;Available from: https://doi.org/10.3390/surfaces5010003.
5. Wang Y, Li Z, Yang D, Qiu X, Xie Y, Zhang X. Microwave-mediated fabrication of silver nanoparticles incorporated lignin-based composites with enhanced antibacterial activity via electrostatic capture effect. J Colloid Interface Sci. 2021; 583:80-8;PMID: 32977194. Available from: https://doi.org/10.1016/j.jcis.2020.09.027.
6. Arshad H, Sadaf S, Hassan U. De-novo fabrication of sunlight irradiated silver nanoparticles and their efficacy against E. coli and S. epidermidis. Sci Reports 2022; 12(1):1-10;PMID: 35027620. Available from: https://doi.org/10.1038/s41598-021-04674-x.
7. Khaydarov RA, Khaydarov RR, Gapurova O, Estrin Y, Scheper T. Electrochemical method for the synthesis of silver nanoparticles. J Nanoparticle Res. 2009;11(5):1193-200;Available from: https://doi.org/10.1007/s11051-008-9513-x.
8. Phuong TNM, Hai NTT, Thuy NTT, Phu NV, Huong NT, Nga DTH, et al. Factors affecting synthesis of silver-nanoparticles and antimicrobial applications. Hue Univ J Sci Nat Sci. 2020;129(1D):25-31;Available from: https://doi.org/10.26459/hueunijns.v129i1D.5955.
9. Wiley BJ, Im SH, Li ZY, McLellan J, Siekkinen A, Xia Y. Maneuvering the surface plasmon resonance of silver nanostructures through shape-controlled synthesis. J Phys Chem B. 2006; 110(32):15666-75;PMID: 16898709. Available from: https://doi.org/10.1021/jp0608628.
10. Shu Z, Kemper F, Beckert E, Eberhardt R, Tünnermann A. Highly sensitive on-chip fluorescence sensor with integrated fully solution processed organic light sources and detectors. RSC Adv. 2017; 7(42):26384-91;Available from: https://doi.org/10.1039/C7RA03841K.
11. Hakkel KD, Petruzzella M, Ou F, van Klinken A, Pagliano F, Liu T, et al. Integrated near-infrared spectral sensing. Nat Commun 2022; 13(1):1-8;PMID: 35013200. Available from: https://doi.org/10.1038/s41467-021-27662-1.
12. Tran N, Phuong T, Xoan T, La N, Tran N, Gia L. Spectrochimica Acta Part A : Molecular and Biomolecular Spectroscopy Rapid and sensitive detection of Rhodamine B in food using the plasmonic silver nanocube-based sensor as SERS active substrate. Spectrochim Acta Part A Mol Biomol Spectrosc. 2021;263:120179;PMID: 34298280. Available from: https://doi.org/10.1016/j.saa.2021.120179.
13. Thi Huong V, Thi Ta HK, Mai NXD, Van Tran TT, Khuyen BX, Trinh KTL, et al. Development of a highly sensitive sensor chip using optical diagnostic based on functionalized plasmonically active AuNPs. Nanotechnology. 2021;32(33):335505;PMID: 33979787. Available from: https://doi.org/10.1088/1361-6528/ac0080.
14. Tu MH, Sun T, Grattan KTV. LSPR optical fibre sensors based on hollow gold nanostructures. Sensors Actuators B Chem. 2014;191:37-44;Available from: https://doi.org/10.1016/j.snb.2013.09.094.
15. Thi Huong V, Thi Ta HK, Mai NXD, Van Tran TT, Khuyen BX, Trinh KTL, et al. Development of a highly sensitive sensor chip using optical diagnostic based on functionalized plasmonically active AuNPs. Nanotechnology. 2021;32(33):335505;PMID: 33979787. Available from: https://doi.org/10.1088/1361-6528/ac0080.
16. Kyaw HH, Al-Harthi SH, Sellai A, Dutta J. Self-organization of gold nanoparticles on silanated surfaces. Beilstein J Nanotechnol. 2015; 6(1):2345-53;PMID: 26734526. Available from: https://doi.org/10.3762/bjnano.6.242.
17. Shameli K, Ahmad M Bin, Zamanian A, Sangpour P, Shabanzadeh P, Abdollahi Y, et al. Green biosynthesis of silver nanoparticles using Curcuma longa tuber powder. Int J Nanomedicine. 2012; 7:5603-10;PMID: 23341739. Available from: https://doi.org/10.2147/IJN.S36786.
18. Ding S-Y, You E-M, Tian Z-Q, Moskovits M. Electromagnetic theories of surface-enhanced Raman spectroscopy. Chem Soc Rev. 2017; 46(13):4042-76;PMID: 28660954. Available from: https://doi.org/10.1039/C7CS00238F.
19. Hoa N, Tran T, Kim J, Phan TB, Khym S, Ju H. Label-Free Optical Biochemical Sensors via Liquid-Cladding-Induced Modulation of Waveguide Modes. ACS Appl Mater Interfaces. 2017;9:31478-41387;PMID: 28849907. Available from: https://doi.org/10.1021/acsami.7b09252.

20. Tran VT, Yoon WJ, Lee JH, Ju H. DNA sequence-induced modulation of bimetallic surface plasmons in optical fibers for sub-ppq (parts-per-quadrillion) detection of mercury ions in water. J Mater Chem A. 2018;6(46):23894-23902;Available from: https://doi.org/10.1039/C8TA08300B.
21. Anker JN, Hall WP, Lyandres O, Shah NC, Zhao J, Van Duyne RP. Biosensing with plasmonic nanosensors. Nat Mater |. 2008;7:442-53;Available from: https://doi.org/10.1038/nmat2162.
22. Wang Y, Zhou J, Li J. Construction of Plasmonic Nano-Biosensor-Based Devices for Point-of-Care Testing. Small Methods. 2017;1(11):1-13;Available from: https://doi.org/10.1002/smtd.201700197.